Temperature Dependence of the Structural Dimensions of the Inverted Hexagonal (H_{II}) Phase of Phosphatidylethanolamine-Containing Membranes†

Mark W. Tate and Sol M. Gruner*

Joseph Henry Laboratories, Department of Physics, Princeton University, Princeton, New Jersey 08544

Received October 18, 1988; Revised Manuscript Received January 30, 1989

ABSTRACT: The characteristic temperature dependence of the lattice basis vector length d of phospholipid–water systems in the inverted hexagonal (H_{II}) phase has been investigated with X-ray diffraction. For 1,2-dioleoyl-*sn*-glycero-3-phosphoethanolamine (DOPE), d falls sharply from 78.1 Å at 10 °C to 62.5 Å at 90 °C. When used in conjunction with the volume fractions of the constituents, d can be used to determine the dimensions within the lipid and water regions. These data showed that a reduction in the radius of the H_{II}-phase water cylinders R_w accounted for most of the reduction in d. From geometrical relationships between the dimensions in the H_{II} phase, it was shown that both d and R_w are sensitive functions of the thickness of the lipid monolayer $d_{H_{II}}$. The characteristic shape of $d(T)$ could be parameterized with the small temperature dependence of $d_{H_{II}}$ along with the ratio v/a, which is the ratio of the specific volume to the area per lipid molecule at the polar interface. The ratio v/a was found to be independent of temperature for the fully hydrated H_{II} system. Additional measurements made with a mixture of DOPE and 1,2-dioleoyl-*sn*-glycero-3-phosphocholine (DOPC), mole ratio 5.07:1, produced a similar parameterization of $d(T)$. The larger basis vector lengths for this mixture compared to those for DOPE can be attributed to a smaller ratio of v/a, which was also found to be temperature independent for this mixture. The smaller value of v/a is due to the larger effective headgroup area of DOPC. The family of $d(T)$ curves produced with differing values of v/a corresponds closely to the nearly parallel family of curves produced by different mixtures of DOPE and DOPC.

The many different phospholipid species occurring in biological membranes have been shown to exhibit a wide variety of polymorphic behavior in the presence of a polar solvent such as water (Cullis et al., 1985). However, the factors responsible for the formation of the phases are often only understood in a limited, qualitative fashion. This is especially true for the nonlamellar phases such as the inverted hexagonal (H_{II}) phase.[1] One striking feature observed in the H_{II} phase is the large decrease of the basis vector length d of the hexagonal lattice with increasing temperature (Figure 1). Many different lipid species have this same characteristic shape of d vs T (Kirk & Gruner, 1985; Tate & Gruner, 1987; Gruner et al., 1988). In particular, Kirk and Gruner (1985) noted that mixtures of DOPE and DOPC in different ratios produce a family of nearly parallel curves of d vs T (see Figure 7). The similarity of the curves leads one to speculate that the curves could be described by only a few parameters.

The H_{II} phase consists of tubes of water arranged on a hexagonal lattice (Figure 1). Lipid monolayers are wrapped around each water core with the polar headgroups of the lipid molecules at the water interface and the hydrocarbon chains filling the interstitial matrix. The basis vector length, d, is the distance between adjacent water cores. An understanding of the behavior of $d(T)$ will involve understanding how both the lipid and water regions within the liquid crystal change with temperature.

Qualitatively, one expects much of the reduction in the size of the H_{II} lattice to be due to a reduction in R_w, the radius of the water core within the H_{II} lattice (Kirk & Gruner, 1985). If this were not the case, the lipid region, of thickness $d_{H_{II}}$, would have to thin approximately by half, causing a corresponding increase in the surface area of the molecule at the water interface, which is likely to be very unfavorable energetically (Israelachvilli et al., 1980). This is not to say that the lipid region is of constant thickness as the temperature is increased, however. One can expect a small decrease in the thickness due to the increasing number of gauche rotamers within the hydrocarbon chains, as has been observed for the case of lipid in the lamellar (L_α) phase (Luzzati, 1968; Seddon et al., 1983).

The rotamers which exist within the melted hydrocarbon chains also introduce a lateral splay within the hydrocarbon region, giving the lipid monolayer a tendency to curl. Kirk et al. (1984) quantified this tendency to curl by introducing a spontaneous radius of curvature R_0 in their treatment of the lyotropic L_α–H_{II} phase transition. A monolayer whose radius of curvature deviates from R_0 will have a curvature free energy associated with it. This is an extension of earlier work treating the curvature energy of a *bilayer* (Deuling & Helfrich, 1976). For cylinders and planes, the curvature free energy is of the form

$$\mu_{curv} = \frac{k_0}{2}\left(\frac{1}{R} - \frac{1}{R_0}\right)^2$$

where k_0 is the bending modulus or rigidity of the monolayer and R is the radius of curvature. In the H_{II} phase, $R \cong R_w$, whereas $R \cong \infty$ in the lamellar phase. An experimental

† This work was supported by the National Institutes of Health (Grant GM32614) and the Department of Energy (Grant DE-FG02-87ER60522-A000). In addition, M.W.T. was supported by a Liposome Company Fellowship. Portions of this work have also been described in Chapter 4 of Tate (1987).

* To whom correspondence should be addressed.

[1] Abbreviations: H_{II}, inverted hexagonal phase; L_α, lamellar phase; R_0, spontaneous radius of curvature; R_w, radius of the water core in the H_{II} phase; d, basis vector length; $d_{H_{II}}$, monolayer thickness in the H_{II} phase; v, specific volume of a lipid molecule; a, interfacial area of a lipid molecule; ϕ_l, lipid volume fraction; ϕ_w, water volume fraction; ϕ_{lim}, lipid volume fraction at limiting hydration; DOPE, 1,2-dioleoyl-*sn*-glycero-3-phosphoethanolamine; DOPC, 1,2-dioleoyl-*sn*-glycero-3-phosphocholine.

0006-2960/89/0428-4245$01.50/0

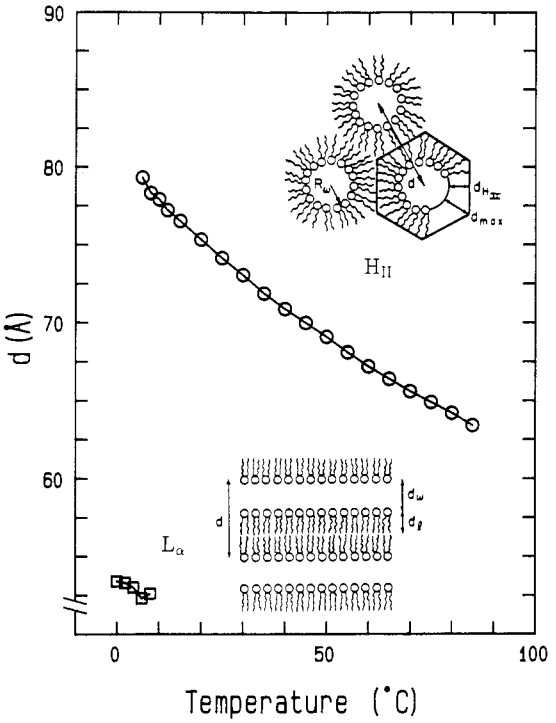

FIGURE 1: Basis vector lengths, d (see inset), for DOPE as determined by X-ray diffraction. The squares at low temperature are used to indicate the L_α phase. The circles indicate the H_{II} phase. Note the dramatic decrease of the H_{II} lattice spacing with temperature. Cross sections of the L_α and H_{II} phases are shown in the insets. In the L_α phase, the planar lipid monolayer is of thickness d_l and the water region is of thickness d_w. The lattice bases is $d = 2d_l + d_w$. The H_{II} phase has tubes of water (radius R_w) arranged on a hexagonal lattice, with each tube surrounded by lipid molecules. The nonpolar hydrocarbon tails fill the interstitial spaces of the lattice, taking on a variety of lengths (from $d_{H_{II}}$ to d_{max}). The H_{II} lattice basis is of length $d = 2(d_{H_{II}} + R_w)$.

measurement performed by Gruner et al. (1986) on several lipid systems confirmed this form of the curvature free energy. In addition, it was shown for each system measured that the spontaneous radius of curvature was near the radius of the water core for the *fully hydrated* liquid crystal.

As the temperature is increased, additional gauche rotamers increase the lateral pressure within the hydrocarbon chain region, consequently reducing the value of R_0. The system will respond to a reduction in R_0 with a corresponding reduction in R_w, and hence in d, in an attempt to reduce the curvature free energy. As yet, however, no measurement of R_0 has been made over a wide range of temperatures. The lack of such a measurement has hampered the understanding of the thermotropic phase transition between the L_α and H_{II} phases. It may be possible, however, to use a parameterization of $d(T)$ to deduce a quantitative description of $R_0(T)$, a much simpler procedure than measuring R_0 for a number of different systems at a number of temperatures.

Experimental Procedures

X-ray diffraction was used to determine the lattice dimensions and the phase of the lipid–water systems. Copper Kα X-rays were generated from a Rigaku RU-200 rotating anode X-ray machine equipped with a microfocus cup and were focused via bent mirror optics (Gruner, 1977; Milch, 1983). Two-dimensional diffraction images were collected with the Princeton SIT and SIV area detectors on two independent X-ray beam lines (Gruner, 1977; Reynolds et al., 1978; Gruner et al., 1982a; Milch, 1983). The digital powder diffraction images were azimuthally integrated along an arc ±15° from the meridional axis (Gruner et al., 1982b; Tilcock et al., 1984; Pascolini et al., 1984). X-ray diffraction from the H_{II} phase is characterized by diffraction peaks which are spaced in the ratios of $1:\sqrt{3}:2:\sqrt{7}$ etc. in reciprocal space. Lead stearate (d = 47.46 Å) was used as a calibration of the lattice basis vector lengths. Measurement of d was to ±0.5 Å.

Samples were prepared with the synthetic lipids 1,2-dioleoyl-*sn*-glycero-3-phosphoethanolamine (DOPE) and 1,2-dioleoyl-*sn*-glycero-3-phosphocholine (DOPC), obtained from Avanti Polar Lipids (Birmingham, AL). Lipids were stored in chloroform solution below −80 °C until needed. A stock solution of the DOPE:DOPC = 5.07:1 mixture was prepared by adding a chloroform solution containing DOPC to a known mass of freshly lyophilized DOPE. This mixture was then lyophilized to determine the mass of the DOPC and then solubilized in chloroform to produce a working stock solution. All samples of the DOPE:DOPC = 5.07:1 mixture were then prepared from this stock.

X-ray specimens were prepared in thin-walled glass X-ray capillaries. About 5 mg of lipid was lyophilized directly in a capillary by first evaporating the chloroform under a stream of nitrogen, solubilizing the lipid in about 15 μL of cyclohexane, and transferring this solution into a weighed capillary for lyophilization. Samples remained under vacuum for at least 2 h to remove any residual cyclohexane. Samples were returned to atmospheric pressure with dry nitrogen gas and weighed immediately. Distilled water was added in the appropriate amount and the capillary reweighed. The capillary was then sealed by melting the upper portion of the capillary under a flame. Weighing the capillary after sealing showed a negligible quantity of water was expelled during the sealing process.

Although lyophilization did facilitate the mixing of the lipid and water, it was found that some means of mechanically mixing samples was necessary if the samples were to be made homogeneous in a relatively short period of time. Samples left up to 4 months at 2 °C showed only slight improvement in the degree of homogeneity as observed optically and by X-ray diffraction from various portions of the sample. To retain an accurate knowledge of the composition, mixing was performed only after the capillary was sealed. Effective mixing was accomplished by changing the orientation of the sealed capillary in a small bench-top centrifuge so as to move the lipid from the bottom of the capillary to the top and back again. This process was repeated at least six times. Flow of the lipid within the capillary was found to occur most readily when the mixture was in the L_α phase. This was most easily accomplished in the case of the DOPE samples by freezing the samples and then centrifuging during the thawing process. In addition, the samples were allowed to equilibrate at 2 °C for at least 3 days. Mixing was deemed complete when the sample was uniform in appearance and would produce uniform diffraction throughout its volume.

Once the samples were well mixed, X-ray diffraction was collected from each sample at 5 °C increments in temperature from 10 to 90 °C. Samples were allowed to equilibrate for 30 min at each temperature before the collection of diffraction. Lattice dimensions were not seen to change after 30 min over a period of at least 3 h. Lattice dimensions for several samples were checked upon cooling and agreed with the data obtained upon heating.

Determination of Structural Parameters. To determine the dimensions of the lipid and water regions within the liquid crystal, the technique of Luzzati was used (Luzzati & Husson, 1962; Luzzati, 1968). Here, the specimen mass is assumed

Table I: Basis Vector Length, d (Å), as a Function of Temperature and Lipid Weight Fraction for the DOPE–Water System

	temp (°C)																
ϕ_l	10	15	20	25	30	35	40	45	50	55	60	65	70	75	80	85	90
0.330	78.2	76.8	75.6	74.1	73.0	71.9	70.8	69.8	68.9	68.0	67.0	66.2	65.4	64.6	63.8	63.3	62.5
0.480	78.3	76.8	75.5	74.3	73.1	71.7	70.9	70.1	68.8	67.9	67.2	66.3	65.5	64.6	63.8	63.2	62.5
0.599	78.3	76.7	75.4	74.2	72.9	71.7	70.8	69.8	68.9	67.9	67.1	66.2	65.3	64.6	63.8	63.1	62.6
0.621	79.0	76.8	75.4	74.2	73.0	71.9	71.0	70.0	69.0	68.1	67.2	66.4	65.6	64.7	64.1	63.2	62.8
0.645	77.8	76.4	75.3	73.9	72.9	71.9	70.8	69.9	68.9	68.1	67.2	66.4	65.7	64.7	64.1	63.4	62.8
0.650	78.1	76.7	75.5	74.4	73.1	72.0	71.0	70.1	69.2	68.3	67.3	66.5	65.5	64.8	64.2	63.5	62.8
0.673	77.7	76.5	75.6	74.7	73.2	72.4	71.1	70.3	69.2	68.3	67.5	66.5	65.8	65.0	64.2	63.5	62.8
0.692	77.7	76.6	75.3	74.1	73.0	71.7	70.7	69.8	68.8	67.9	66.9	66.1	65.2	64.6	63.7	63.2	62.3
0.704	77.8	76.5	75.3	74.1	72.8	71.7	70.7	69.8	69.0	68.1	67.0	66.3	65.6	64.8	64.1	63.4	62.5
0.710	76.6	75.8	75.1	74.3	73.0	71.7	70.7	69.7	68.6	67.7	66.8	65.9	65.0	64.2	63.4	62.8	62.1
0.717	75.6	74.7	74.1	73.2	72.7	71.8	70.7	69.9	68.6	67.7	66.7	65.9	65.2	64.1	63.4	62.7	62.2
0.720	75.0	74.2	73.4	72.8	72.1	71.3	70.7	69.6	68.6	67.6	66.5	65.6	64.9	64.1	63.3	62.8	62.3
0.723	74.7	73.5	72.9	72.4	71.9	71.3	70.8	69.8	69.1	68.3	67.1	66.4	65.5	64.5	63.8	63.1	62.5
0.727	74.2	73.4	72.8	72.2	71.7	70.9	70.4	70.1	69.1	68.2	67.1	66.1	65.4	64.4	63.6	62.9	62.3
0.738	73.2	72.5	71.7	71.1	70.7	70.0	69.3	69.0	68.4	67.7	67.0	65.9	65.2	64.2	63.4	62.7	62.1
0.754	71.6	70.9	70.1	69.5	69.1	68.4	67.8	67.3	66.7	66.3	65.8	65.3	64.7	64.1	63.3	62.6	61.9
0.768	69.8	68.6	68.1	67.3	66.8	66.2	65.6	65.2	64.6	64.1	63.7	63.1	62.8	62.3	61.9	61.2	60.7
0.778	69.5	67.7	66.0	64.9	64.1	63.4	63.0	62.6	62.2	61.8	61.4	61.0	60.7	60.4	60.1	59.7	59.5
0.808		64.2	61.4	60.7	60.2	59.7	59.2	58.9	58.3	57.9	57.4	56.9	56.5	56.0	55.5	55.0	54.4
0.856			56.2	55.7	55.5	54.9	54.4	54.0	53.5	53.1	52.7	52.1	51.5	51.0	50.7	50.1	49.9

to be partitioned into distinct water and lipid regions. The dimensions of each region then follow simply from the basis vector length, determined through X-ray diffraction, if the volume fraction of each constituent within the liquid crystal is known.

In the H_{II} phase (Figure 1), the basis vector length d is given by

$$d = 2(d_{H_{II}} + R_w) \quad (1)$$

where $d_{H_{II}}$ is the thickness of the lipid monolayer along the direction between adjacent water tubes and R_w is the radius of the water core, which is assumed to be cylindrical. Knowing the volume fraction of water ϕ_w and the basis vector length, the radius of the water core is

$$R_w = d\sqrt{\phi_w\sqrt{3}/2\pi} \quad (2)$$

The area a which the lipid occupies at the lipid–water interface can be found from

$$\frac{v}{a} = \frac{d}{2}\frac{1-\phi_w}{\sqrt{\phi_w 2\pi/\sqrt{3}}} \quad (3)$$

where v is the volume of a single lipid molecule. The maximum length which a lipid molecule must stretch d_{max} for the lipid to completely fill the interstitial spaces (see Figure 1) is given by

$$d_{max} = \frac{d}{\sqrt{3}} - R_w \quad (4)$$

Note the difference between d_{max} and $d_{H_{II}}$ is

$$d_{max} - d_{H_{II}} = d\left(\frac{1}{\sqrt{3}} - \frac{1}{2}\right) \quad (5)$$

which depends only on the size of the lattice, not on the size of the water core.

If two phases coexist, as allowed by the Gibbs phase rule for a two-component system, then the volume fraction of each constituent in each of the phases will in general not be known. Of particular interest in this paper are the dimensions of the lipid and water regions of the liquid crystal under the condition that the liquid crystal is coexisting with a bulk water phase. X-ray diffraction from the liquid crystalline phase will show a constant lattice size as long as the bulk water phase is present. At water concentrations below the limiting hydration, the dimensions of the water region within the liquid crystal will be reduced, causing the X-ray spacing to be diminished also. To determine the point of limiting hydration, the X-ray spacings from a series of samples of varying water content were fit to a function which was constant above the excess water fraction and decreased linearly for a reasonable range below that fraction.

Volume fractions of the lipid and water were found from the known mass ratio of the lipid–water mixture in conjunction with the densities of the constituents. We assume that the density of each constituent in the mixture is the same as its bulk value (White et al., 1987). The density of DOPE in the H_{II} phase was measured by a neutral buoyancy technique (Nagle & Wilkinson, 1978). Lipid added to water–deuterium oxide mixtures of different ratios was centrifuged at each of four temperatures between 10 and 50 °C, noting the density of the H_2O–D_2O mixture at which the lipid becomes buoyant. This yielded a density for DOPE of 1.026, 1.015, 1.006, and 0.999 g/mL at 10, 25, 35, and 50 °C, respectively. Densities at other temperatures were found from the linear fit to these data points. The density of the DOPE–DOPC mixture was assumed to be the same as that for DOPE.

Results

DOPE. The basis vector length, d, for a series of DOPE samples with varying water content was measured as a function of temperature by X-ray diffraction (Table I). Figure 2 shows d as a function of lipid fraction for three representative temperatures for which it was measured. At constant temperature, a sharp reduction in d is observed when the water fraction is reduced below the limiting value. The volume fraction of the lipid at limiting hydration, ϕ_{lim}, is seen to increase considerably from 68.9% at 10 °C to 75.7% at 90 °C (Figure 3).

Having determined $\phi_{lim}(T)$ as well as $d(T)$ at full hydration, the internal dimensions of the H_{II} phase of a sample with an excess of water can be calculated (Figure 3 and Table II). These data show that, indeed, most of the temperature variation in the size of the H_{II} lattice is due to a reduction in the radius of the water core, as R_w falls from 22.9 Å at 10 °C to 16.2 Å at 90 °C. Over the same temperature range, $d_{H_{II}}$ decreases only by ~1 Å, from 16.2 Å at 10 °C to 15.1 Å at 90 °C. The area of the lipid molecule at the water interface is seen to increase slightly with temperature, from 47.5 Å^2 at 10 °C to 50.6 Å^2 at 90 °C. Note, however, that the ratio v/a

Table II: Dimensions of the H_{II} Phase as a Function of Temperature for the Fully Hydrated DOPE System

T (°C)	d (Å)	ϕ_{lim}	R_w (Å)	$d_{H_{II}}$ (Å)	d_{max} (Å)	ν/a (Å)	a (Å^2)
10	78.1	0.689	22.9	16.2	22.2	25.4	48
15	76.6	0.695	22.2	16.1	22.0	25.3	48
20	75.4	0.704	21.6	16.2	22.0	25.6	47
25	74.2	0.709	21.0	16.1	21.8	25.6	48
30	73.0	0.715	20.5	16.0	21.7	25.7	48
35	71.9	0.718	20.0	15.9	21.5	25.5	48
40	70.7	0.726	19.5	15.9	21.4	25.7	48
45	69.9	0.732	19.0	15.9	21.3	25.9	48
50	68.9	0.737	18.5	15.9	21.2	26.0	48
55	68.0	0.741	18.2	15.8	21.1	25.9	48
60	67.0	0.744	17.8	15.7	20.9	25.9	48
65	66.2	0.746	17.5	15.6	20.7	25.7	48
70	65.4	0.748	17.2	15.5	20.5	25.6	49
75	64.6	0.751	16.9	15.4	20.4	25.5	49
80	63.8	0.754	16.6	15.3	20.2	25.5	50
85	63.1	0.754	16.4	15.1	20.0	25.2	50
90	62.5	0.757	16.2	15.1	19.9	25.2	51

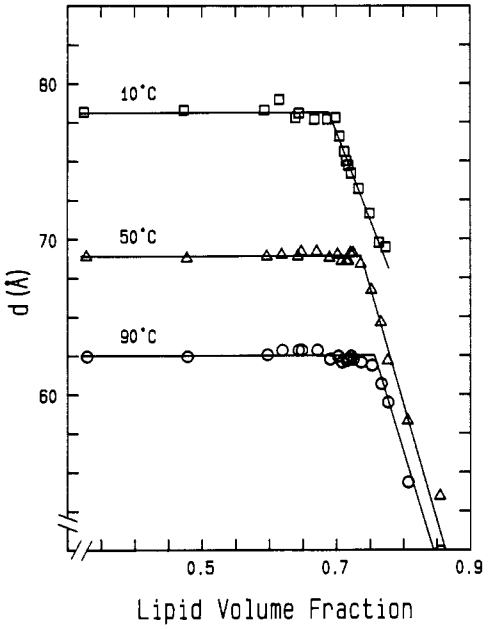

FIGURE 2: DOPE H_{II} basis vector length as a function of lipid volume fraction at 10, 50, and 90 °C. The lines show the fit to the data used to obtain ϕ_{lim}. Below ϕ_{lim}, the fitted function is a constant. Above ϕ_{lim}, a linear dependence on ϕ_l is assumed.

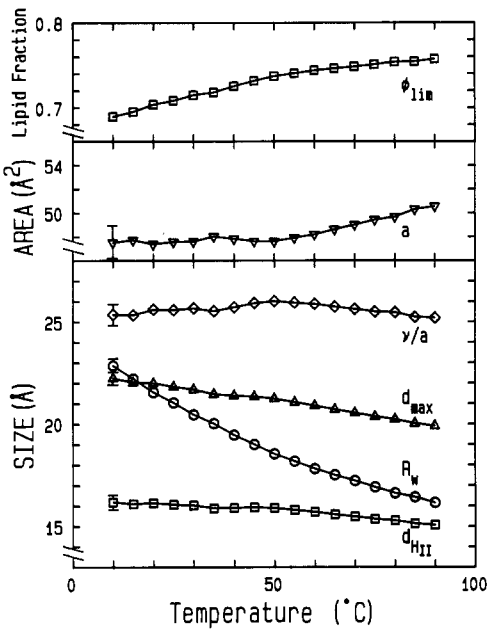

FIGURE 3: Structural parameters at limiting hydration for DOPE. Shown are ϕ_{lim}, a, $d_{H_{II}}$, R_w, d_{max}, and ν/a. Representative error bars are shown on the first data points. The error in ϕ_{lim} is the same as the size of the symbol. The reduction of the H_{II} lattice with temperature can be seen here to be mainly attributed to the corresponding reduction in the size of the water core. The thickness of the lipid annulus, $d_{H_{II}}$, decreases only by ~1 Å over the temperature range studied (10–90 °C). Although both the volume of the lipid molecule and its interfacial area are changing with temperature, the ratio, ν/a, is seen to remain fairly constant over the temperatures studied.

is constant to within experimental error over the entire temperature range.

When compared to measurements made in the L_α phase, $d_{H_{II}}$ is seen to be smaller than the thickness of a DOPE monolayer in the L_α phase (18.5 Å at 2 °C; Gruner et al., 1988). Note, however, that $d_{H_{II}}$ is the minimum thickness of the monolayer in the H_{II} phase. The maximum length, d_{max}, is greater than the lamellar monolayer thickness (d_{max} = 22.2 Å at 10 °C and 19.9 Å at 90 °C). Taking a weighted average of the monolayer thickness in the H_{II} phase at 10 °C yields a thickness of 18.1 Å, only slightly less than the lamellar thickness. There is, however, a pronounced difference in a between the H_{II} and L_α phases. The area in the H_{II} phase is much less than the value of 65 Å^2 measured for DOPE in the L_α phase at 2 °C (Gruner et al., 1988).

Also of interest is the behavior of the internal dimensions for samples at reduced hydrations (Figure 4). Dimensions which are given for excess water samples are calculated from the value of ϕ_{lim} found at that temperature. Both R_w and the ratio ν/a are seen to depend strongly on ϕ_l. At 50 °C, R_w decreases from 18.6 Å at 72% lipid to 13.5 Å at 80.8%. As the lipid fraction is increased, ν/a increases sharply due to a reduction in a. In contrast, $d_{H_{II}}$ is seen to have very little dependence on lipid concentration. At 10 °C, $d_{H_{II}}$ does increase as the water content is reduced (Figure 4). However, for all temperatures above 15 °C, $d_{H_{II}}$ is seen to be constant with concentrations of water down to at least 15%. At these temperatures, the result of limited hydration is a decrease in the area of the lipid at the interface and smaller water cores without greatly affecting the length of the molecule. This suggests that much more energy is required to change its length than to change the cross-sectional area. Note that in the lamellar phase ν/a and the thickness of the monolayer are coupled directly through the geometry of the phase, suggesting that much of the resistance to lateral compressibility in the lamellar phase results from the resistance of the hydrocarbon chains to change their length.

Parameterization of d vs T. The large reduction in R_w with increasing temperature can be explained by a corresponding decrease in the spontaneous radius of curvature. The spontaneous curvature of the lipid monolayer comes from the en-

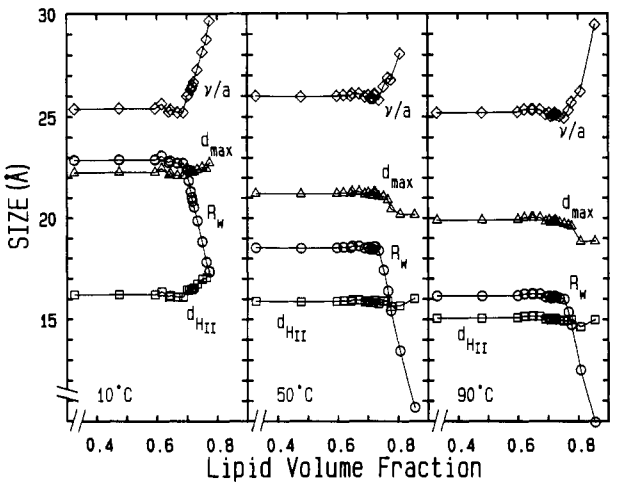

FIGURE 4: Internal dimensions of the H_{II} phase of DOPE as a function of the lipid concentration at 10, 50, and 90 °C. R_w and ν/a each have a strong dependence on the lipid concentration, while $d_{H_{II}}$ and d_{max} change little. $d_{H_{II}}$ is seen to be roughly constant as the lattice is dehydrated at 50 and 90 °C (also at other temperatures not included in this figure). At 10 °C, $d_{H_{II}}$ is seen to increase slightly as the water is removed.

tropic splay within the hydrocarbon region (which increases with temperature) coupled with the effective size of the polar headgroup. The internal dimensions measured for lipid region should be a measure of the splay within a molecule and, hence, a measure of the spontaneous curvature. However, the dimensions of the lipid region are changing only slightly over the temperature range measured. Thus with only small changes in one region, that is, small changes in $d_{H_{II}}$ and a, large changes are induced in the other, seen as a large reduction in R_w. To explain this in a quantitative manner, another look at the geometry of the H_{II} phase is in order to develop relationships between the internal dimensions.

Consider a hexagonal two-dimensional Wigner–Seitz unit cell of the H_{II} lattice of length l centered around a water cylinder (Figure 1). The volume of this cell is

$$V_{cell} = 2\sqrt{3}(d_{H_{II}} + R_w)^2 l$$

and the volume of the lipid and water regions are

$$V_l = l(2\sqrt{3}(d_{H_{II}} + R_w)^2 - \pi R_w^2)$$

and

$$V_w = l\pi R_w^2$$

The total surface area at the lipid–water interface is

$$A = 2\pi R_w l$$

If N is the number of lipid molecules within the unit cell, then the volume per lipid molecule ν is

$$\nu = V_l/N$$

while the area per lipid molecule at the interface is

$$a = 2\pi R_w l/N$$

Taking the ratio of ν to a gives

$$\frac{\nu}{a} = \frac{2\sqrt{3}(d_{H_{II}} + R_w)^2 - \pi R_w^2}{2\pi R_w}$$

Solving for R_w we find

$$R_w = [(\pi\nu/a - 2\sqrt{3}d_{H_{II}}) \pm \sqrt{(\pi\nu/a - 2\sqrt{3}d_{H_{II}})^2 - 2\sqrt{3}(2\sqrt{3} - \pi)d_{H_{II}}^2}]/(2\sqrt{3} - \pi) \quad (6)$$

The larger root will be unfavored due to the increased free energy associated with packing the lipid into the interstitial spaces of a larger structure (Kirk et al., 1985). The lattice spacing d as a function of $d_{H_{II}}$ and ν/a can be found by substituting eq 6 into eq 1.

In contrast to the H_{II} phase, the thickness of the water region in the lamellar phase has no fixed geometrical relationship to either the thickness of the monolayer, d_l, or ν/a. The thickness of the monolayer, d_l, and ν/a are directly coupled through the geometry of the phase, however. In particular, for a lamellar phase

$$d_l = \frac{\nu}{a} = \phi_l d/2$$

Due to the added degree of freedom of a two-dimensional lattice, however, no direct geometrical relationship of ν/a and $d_{H_{II}}$ exists for the hexagonal phase. Assume then, as a first approximation, that ν/a and $d_{H_{II}}$ are independent of one another. One expects that the length of the lipid molecule will be affected by temperature as more gauche rotamers are introced within the hydrocarbon chain. Although both ν and a might be expected to increase with temperature, the temperature dependence of the ratio ν/a is not obvious a priori. Let us then take as a working assumption that ν/a is constant with temperature. From the data obtained for DOPE, we see that such an assumption is not unreasonable, as the increases in ν and a cancel one another to within our experimental error (Figure 3). It is important to recognize that constant ν/a holds only for the fully hydrated lipid system. At constant water fractions below excess, ν/a decreases significantly with temperature.

Figure 5 shows d as a function of $d_{H_{II}}$ for constant ν/a from eq 6. Note that the $d_{H_{II}}$ axis is inverted. Each curve of constant ν/a shows a striking resemblance to the measured $d(T)$ of the H_{II} phase. Obtaining the functional form of $d_{H_{II}}(T)$ will provide the form of d vs T (or, alternatively, R_w vs T), since eq 1 and 6 together are functions of $d_{H_{II}}$ and ν/a.

A linear function was found to fit well to $d_{H_{II}}(T)$ over the temperature range studied (Table II). A least-squares fit to the data yields

$$d_{H_{II}}(\text{Å}) = 16.44\ (\pm 0.15) - 0.0139\ (\pm 0.0013) \times T(°\text{C}) \quad (7)$$

Figure 6 shows $d(T)$ obtained by combining eq 1 and 6 together with the linear fit of $d_{H_{II}}$ with temperature given by eq 7. ν/a was assumed to be constant and equal to 25.6 Å, the average of the measured values (Figure 3). There are no free parameters in this fit. Shown for comparison are the lattice spacings measured for DOPE. A linear decrease in $d_{H_{II}}$ with temperature and a constant value of ν/a provide a simple parameterization of both d and R_w as a function of temperature.

Internal Dimensions for DOPE–DOPC Mixtures. Addition of DOPC to DOPE has been shown to increase the L_α–H_{II} transition temperature T_{bh}, with increasing mole fraction of DOPC (Figure 7; Kirk & Gruner, 1985; Tate & Gruner, 1987). Also, as noted in the introduction, the H_{II} phase basis vector lengths from mixtures of DOPE and DOPC appear to form a family of curves of $d(T)$ with d increasing as the DOPC fraction increases. The basis vector length in the lamellar phase is also seen to increase monotonically with DOPC fraction as well (Kirk & Gruner, 1985). Since both species of lipid have the same oleic chains, changes in the phase behavior and lattice spacings ultimately result from headgroup effects.

In the L_α phase, the difference between the lattice spacings of DOPE and DOPC can be attributed to an increased hy-

Table III: Dimensions for the Fully Hydrated DOPE:DOPC = 5.07:1 System in the H_{II} Phase

T (°C)	d (Å)	ϕ_{lim}	R_w (Å)	$d_{H_{II}}$ (Å)	d_{max} (Å)	ν/a (Å)	a (Å²)
50	73.5	0.691	21.5	15.3	21.0	24.0	52
70	70.3	0.701	20.2	15.0	20.4	23.7	54
90	67.4	0.716	18.9	14.8	20.1	23.8	54

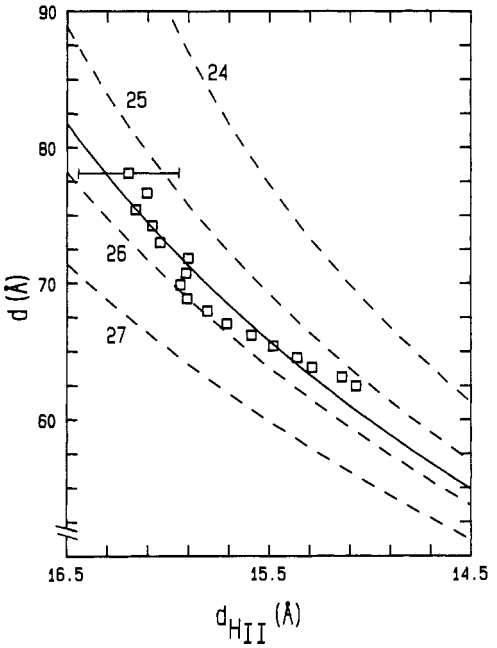

FIGURE 5: H_{II} basis vector length, d, as a function of $d_{H_{II}}$ for constant values of ν/a. The value of ν/a for each curve is indicated in the figure. These curves are computed from purely geometrical relationships (see text). Note that the $d_{H_{II}}$ axis is inverted. The data points included are those measured for DOPE in excess water. The solid line is the curve with ν/a equal to the average of the values measured for DOPE. The meandering of the data points is believed to be due to residual systematic error in the determination of $d_{H_{II}}$. Note representative error bar.

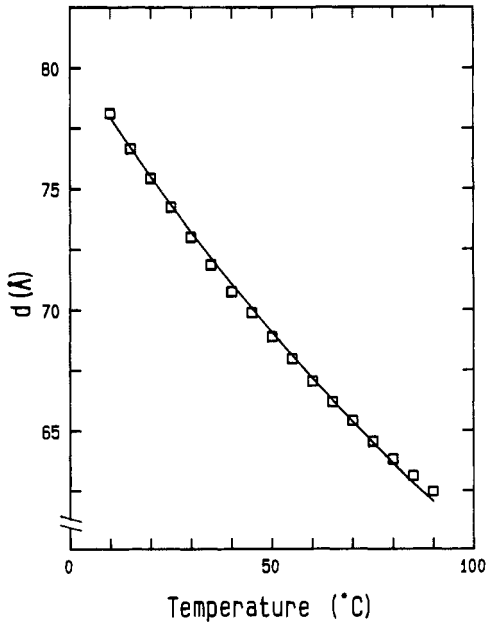

FIGURE 6: Temperature dependence of a fully hydrated H_{II} phase in the DOPE–water system. The solid curve represents spacings calculated by assuming $d_{H_{II}}$ has a linear dependence on temperature and ν/a is constant, and equal to the average of the measured values.

dration repulsion between lipid bilayers for DOPC [e.g., see Rand (1981) and Gruner et al. (1988)]. The DOPE headgroups hydrogen bond more strongly with each other, allowing for less perturbation of the water layer, which in turn results

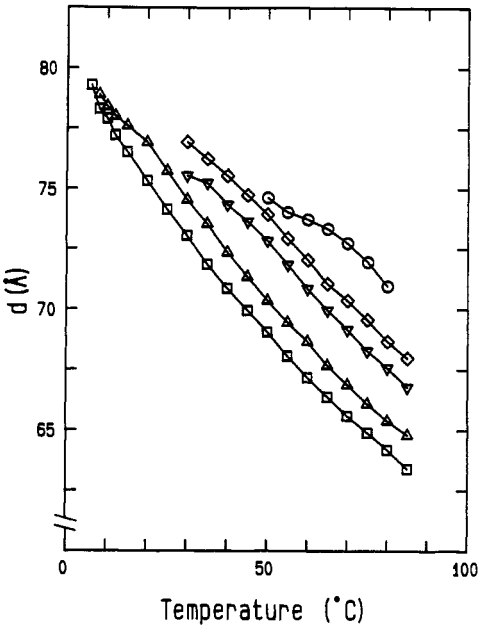

FIGURE 7: H_{II} basis vector lengths for a series of DOPE–DOPC mixtures: (□) DOPE; (△) DOPE:DOPC = 23:1; (▽) DOPE:DOPC = 6.34:1; (◇) DOPE:DOPC = 5.07:1; (○) DOPE:DOPC = 3.17:1. Note that in the high-temperature region the curves from each sample are roughly parallel. The curves depart from this parallel nature at the lower temperature end of each curve where a coexisting L_α phase (not indicated in the figure) is seen in addition to the H_{II} lattice. For the DOPE:DOPC = 3.17:1 mixture, the phase coexistence region extends from 50 to 60 °C. Within the coexistence region, the DOPE:DOPC ratio within the separate phases may, in general, be different from the mean. Thus some deviation from the parallel family of curves can be expected in this region.

in a lower hydration repulsion. In addition to bonding together less strongly, the DOPC headgroups are sterically larger due to the substituted methyl groups on the terminal amine of the headgroup. Thus the addition of DOPC to DOPE should increase the average value of a in both the L_α and H_{II} phases, which will lower the ratio of ν/a.

In the H_{II} phase, a change in the ratio of ν/a will manifest itself as a change in the value of d. Equation 6 produces a family of nearly parallel curves of $d(d_{H_{II}})$, each curve corresponding to a different value of ν/a (Figure 5). Since the variation of $d_{H_{II}}$ with DOPC concentration should be small, one expects that the family of $d(T)$ curves which have been observed experimentally for DOPE–DOPC systems should correspond directly to the family of curves produced by eq 6, with each DOPE:DOPC ratio associated with a unique value of ν/a.

Internal dimensions for the mixture of DOPE and DOPC in the mole ratio of 5.07:1 were measured (Table III) according to the method of Luzzati described in the section above. A value of DOPE:DOPC = 5:1 was chosen. This produced X-ray spacings significantly different from those of DOPE while keeping the bilayer–hexagonal transition temperature, T_{bh}, well below 100 °C, thus allowing the temperature dependence of the parameters, as well as the dependence on DOPC fraction, to be measured. The ratio 5.07:1 was determined post priori by measurement of the mass of each constituent added from solution (see Experimental Proce-

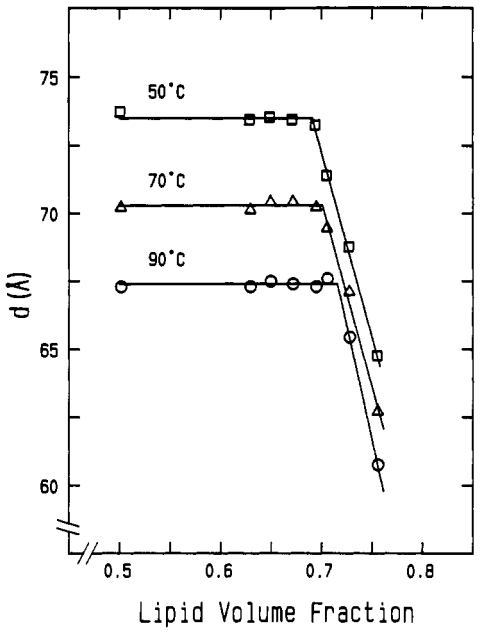

FIGURE 8: Lipid concentration dependence of the H_{II} lattice size for the DOPE:DOPC = 5.07:1 mixture at 50, 70, and 90 °C. See the caption for Figure 2.

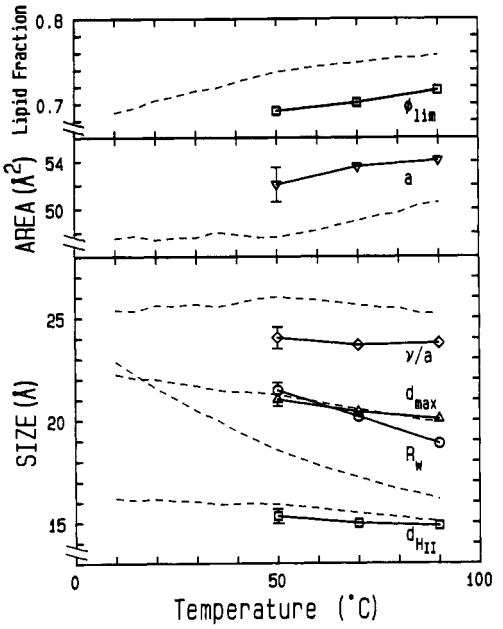

FIGURE 9: Internal dimensions of the fully hydrated DOPE:DOPC = 5.07:1 mixture as a function of temperature. See caption for Figure 3. The dashed lines are the data measured for DOPE and are included for comparison (see Figure 3). The radius of the water core is seen to have increased from that of the pure DOPE case, while $d_{H_{II}}$ and d_{max} have remained virtually unchanged. ν/a is reduced considerably due to the large effective headgroup area of the DOPC molecule.

dures). T_{bh} for a sample with excess water was found to be 30–40 °C, the temperature region over which the L_α and H_{II} phases coexisted for this three-component system. The basis vector length in the H_{II} phase for this fully hydrated sample was about 4 Å greater than d for DOPE at the same temperature.

Figure 8 shows d as a function of ϕ_l at constant temperature. Values for ϕ_{lim} were obtained at 50, 70, and 90 °C and once again used to calculate the internal dimensions of the excess water sample (Figure 9 and Table III). As expected, the thickness of the lipid monolayer, $d_{H_{II}}$, is similar to that of DOPE, only about 0.5 Å less, a change of only 3%. R_w has, however, increased by about 3 Å from the value found for

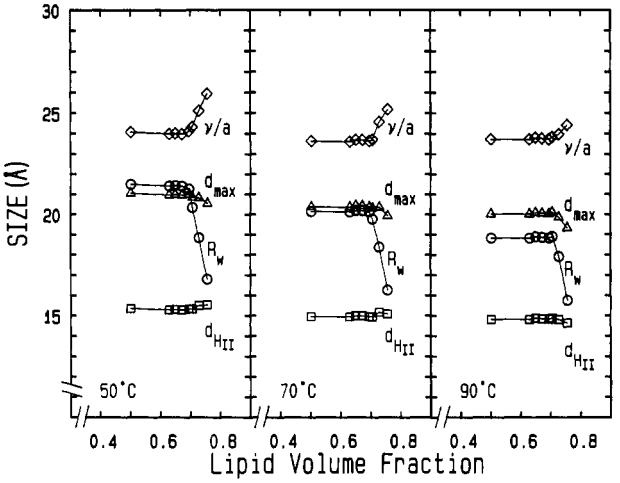

FIGURE 10: Internal dimensions of the H_{II} lattice as a function of lipid concentration for the DOPE:DOPC = 5.07:1 mixture. The figures show essentially the same behavior as was observed for DOPE (Figure 4). Note particularly that $d_{H_{II}}$ is once again relatively insensitive to concentration.

DOPE, a change of 16%. This change in R_w can be related to the change in ν/a, which has decreased, as expected, from the pure DOPE case. At 70 °C, ν/a for the DOPE–DOPC mixture is 23.7 Å compared to 25.6 Å for DOPE. The interfacial area of the DOPE–DOPC mixture at this temperature increased to 53.6 Å² from 49.0 Å² for DOPE due to the larger effective headgroup size of the DOPC molecule.

Again we note that the ratio ν/a for this fully hydrated system is constant with temperature as well. Once again, the $d(T)$ curve can be parameterized with a constant value of ν/a along with a linear variation in $d_{H_{II}}$. The similarity of the values of $d_{H_{II}}(T)$ for the DOPE and DOPE–DOPC systems indicates that the family of nearly parallel curves observed experimentally for all DOPE–DOPC mixtures can be related directly to a family of curves characterized by headgroup-dependent values of ν/a.

Internal dimensions at limited hydrations for the DOPE–DOPC mixture are displayed in Figure 10. These dimensions show qualitatively the same features as the pure DOPE case, as once again $d_{H_{II}}$ is relatively insensitive to variations in the water concentration while R_w and ν/a change rapidly.

Conclusions

The goal of this study was to understand the characteristic thermal variation of the excess water hexagonal basis vector length, $d(T)$. Vital to this understanding is the characterization of the dimensions within the lipid and water regions. Consideration of the geometry of the H_{II} phase, given cylindrical water cores and the absence of vacuum voids, leads to a relationship (eq 6) between the water cylinder radius, R_w, the hydrocarbon thickness, $d_{H_{II}}$, and the specific volume to interfacial area ratio, ν/a. One can use any two of these dimensions to describe the behavior of $d(T)$. Hopefully, the description will be simple as well as give insights into the behavior of lipid in the H_{II} phase.

Although ν and a both vary with temperature, somewhat to our surprise, the ratio of ν/a for DOPE was constant to within experimental error. The beauty of this finding, in view of eq 6, is that once ν/a has been determined, there is a one to one relationship between R_w and $d_{H_{II}}$. Similarly, ν/a was found to be constant for a DOPE:DOPC = 5.07:1 mixture, except that the ratio of ν/a for this mixture was different than that for DOPE. The smaller value for the mixture is expected due to the effectively larger PC headgroups. The characteristic

family of nearly parallel $d(T)$ curves found with lipids with similar chains [Figure 7; see also Figure 7 of Kirk and Gruner (1985) and Figure 9 of Gruner et al. (1988)] is largely a consequence of different v/a values for the different systems.

It is important to note that, for the fixed v/a value typical of H_{II} phases, $d = 2(R_w + d_{H_{II}})$ is, by eq 6, a very sensitive function of $d_{H_{II}}$. This is simply a consequence of the hexagonal geometry. For DOPE, a variation in d of almost 16 Å, from 10 to 90 °C, results from a variation in $d_{H_{II}}$ of only about 1.1 Å. The data are well fit by a simple linear variation of $d_{H_{II}}$ with temperature with a modest temperature coefficient of −0.0139 Å/°C. The choice of $d_{H_{II}}$ to parameterize $d(T)$ is appealing due to not only its simple temperature dependence but the intuitive physical basis of the temperature dependence due to the polymer-like properties of the hydrocarbon chains.

One can fully characterize the $d(T)$ curve of DOPE by three numbers: v/a, the thickness of $d_{H_{II}}$ at an arbitrary temperature, and the (negative) coefficient of thermal expansion of $d_{H_{II}}$. Measurement of these three numbers yields a theoretical $d(T)$ curve which has no remaining free parameters and is in good agreement with the measured $d(T)$ curve (Figure 6). We speculate that families of $d(T)$ curves for diverse lipid systems may be characterized by different values of these three numbers.

A more fundamental description of $d(T)$ would be in terms of the temperature dependence of free energy parameters such as R_0. Gruner et al. (1986) were able to measure the work necessary to deform a lipid monolayer to a different radius of curvature by measuring the dimensions of the lipid and water regions within the H_{II} phase as a function of osmotic stress applied to the system. The results not only confirmed that the form for the curvature free energy used by Kirk et al. (1984) was valid over a large range of radii but showed that for all the systems studied the spontaneous radius of curvature was approximately equal to the radius of the water core in the *fully* hydrated H_{II} phase. If $R_0 \cong R_w$ for H_{II} phases in general, the task of measuring R_0 for each system becomes greatly simplified (Gruner et al., 1988). Parameterizing $R_w(T)$ in terms of $d_{H_{II}}$ and v/a will simplify this process even more.

Although R_0 was not explicitly measured over a wide range of temperatures (Gruner et al., 1986), an argument can be made to generalize the statement that $R_0 \cong R_w$ for other temperatures. It is possible that some free energy term exists which could cause the actual radius of curvature, R_w, to be different than the spontaneous radius of curvature. One such free energy is the hydrocarbon packing free energy proposed by Kirk et al. (1984). They show that the magnitude of this term in the H_{II} geometry increases as the size of the unit cell increases. Minimizing the total free energy of the H_{II} phase will result in a compromise between the free energy terms, resulting in a reduction of the radius of the water core from R_0. This effect should be most pronounced at low temperatures where the largest lattices are seen. The addition of free alkanes, such as dodecane, to DOPE is seen to relieve the packing constraints in the H_{II} phase, causing the L_α–H_{II} transition temperature to be lowered dramatically (Kirk & Gruner, 1985). The reduction in packing constraints should also allow R_w to relax toward R_0. The resulting lattice spacing of a sample with dodecane is only ~1 Å larger than that from a sample without the alkane (Tate & Gruner, 1987; Tate, 1987), implying that $R_w \cong R_0$ holds for the low-temperature cases as well.

To show that added dodecane was not in itself modifying the spontaneous curvature, Gruner et al. (1986) used the osmotic stress technique on a system with alkane as well. They found that R_0 values with and without the added dodecane were within 1 Å of one another. Dodecane has been added to a myriad of lipids which exhibit the H_{II} phase, in each case having a similar effect: lowering T_{bh} considerably while having little effect on the basis vector length in the H_{II} phase (Kirk & Gruner, 1985; Tate & Gruner, 1987; Gruner et al., 1988; unpublished data from this laboratory).

The parameterization of $d(T)$ should simplify gathering information on $R_0(T)$ for a variety of systems other than those measured here. Estimates from systems which are similar in some respect to the DOPE and the DOPE–DOPC systems studied can be easily made. For example, DOPE–Me, which also has oleic chains, has a different lattice basis vector length in the H_{II} phase than DOPE. From the measurement of d alone, one can estimate values for R_w and v/a, assuming that the behavior of $d_{H_{II}}(T)$ is the same for the DOPE–Me system. At 70 °C, d for DOPE–Me is 74.1 Å, giving estimated values for R_w and v/a of 21.6 Å and 24.3 Å, respectively. For systems which are not similar to DOPE, measurement of $d_{H_{II}}$ and v/a at one or two temperatures should be sufficient to parameterize $R_w(T)$.

Even though the curvature in the L_α phase is essentially zero, Kirk et al. (1984) showed that the curvature energy of a monolayer in the L_α phase can be considerable. The spontaneous curvature, which is assumed to be an intrinsic property of the monolayer, may have a value significantly different from zero even while the system is in the lamellar phase. Using the parameterization found here, one should be able to estimate the value of R_0 in the L_α phase by extrapolating from data gathered in the H_{II} phase.

The parameterization presented here should be tested for other systems which exhibit the H_{II} phase; in particular, the observation that v/a is constant at full hydration should be examined. Gaining a measure of R_0 and other quantities associated with the free energy of lipid–water systems is important to advancing the theory of the phase transitions of nonlamellar phases. An improvement on the phenomenological description of $R_0(T)$ awaits a functional form of $d_{H_{II}}(T)$ obtained from molecular models and a direct calculation of R_0 of a free monolayer from such models.

Acknowledgments

We thank E. Shyamsunder and D. Turner for their helpful input during the course of the experiments.

Registry No. DOPC, 4235-95-4; DOPE, 2462-63-7.

References

Cullis, P. R., Hope, M. J., de Kruijff, B., Verkleij, A. J., & Tilcock, C. P. S. (1985) in *Phospholipids and Cellular Regulations* (Kuo, J. F., Ed.) Vol. I, pp 1–59, CRC Press, Boca Raton, FL.

Deuling, H. J., & Helfrich, W. (1976) *Biophys. J. 16*, 861–868.

Gruner, S. M. (1977) *The Application of an Efficient X-ray Detector to Diffraction from Retinal Rod Outer Segment Membranes*, Ph.D. Thesis, Princeton University, Princeton, NJ.

Gruner, S. M., Milch, J. R., & Reynolds, G. T. (1982a) *Rev. Sci. Instrum. 53*, 1770–1778.

Gruner, S. M., Milch, J. R., & Reynolds, G. T. (1982b) *Nucl. Instrum. Methods Phys. Res. 195*, 287–297.

Gruner, S. M., Parsegian, V. A., & Rand, R. P. (1986) *Faraday Discuss. Chem. Soc. 81*, 29–37.

Gruner, S. M., Tate, M. W., Kirk, G. L., So, P. T. C., Turner, D. C., Keane, D. T., Tilcock, C. P. S., & Cullis, P. R. (1988) *Biochemistry 27*, 2853–2866.

Israelachvili, J. N., Marcelja, S., & Horn, R. G. (1980) *Q. Rev. Biophys. 13*, 121–200.
Kirk, G. L. (1984) *Thermodynamic Models and Experimental Investigations of the Lamellar (L_α) to Inverse Hexagonal (H_{II}) Phase Transition of Lipid–Water Systems*, Ph.D. Thesis, Princeton University, Princeton, NJ.
Kirk, G. L., & Gruner, S. M. (1985) *J. Phys. 46*, 761–769.
Kirk, G. L., Gruner, S. M., & Stein, D. L. (1984) *Biochemistry 23*, 1093–1102.
Luzzati, V. (1968) *Biol. Membr. 1*, 71–123.
Luzzati, V., & Husson, F. (1962) *J. Cell Biol. 12*, 207–219.
Milch, J. R. (1983) *J. Appl. Crystallogr. 16*, 198–203.
Nagel, J. F., & Wilkinson, D. A. (1978) *Biophys. J. 23*, 159–175.
Pascolini, D., Blasie, J. K., & Gruner, S. M. (1984) *Biochim. Biophys. Acta 777*, 9–20.
Rand, R. P. (1981) *Annu. Rev. Biophys. Bioeng. 10*, 277.
Reynolds, G. T., Milch, J. R., & Gruner, S. M. (1978) *Rev. Sci. Instrum. 49*, 1241–1249.
Seddon, J. M., Cevc, G., & Marsh, D. (1983) *Biochemistry 22*, 1280–1289.
Tate, M. W. (1987) *Equilibrium and Kinetic States of the L_α–H_{II} Phase Transition*, Ph.D. Thesis, Princeton University, Princeton, NJ.
Tate, M. W., & Gruner, S. M. (1987) *Biochemistry 26*, 231–236.
White, S. H., Russell, E. J., & King, G. I. (1987) *Biophys. J. 52*, 663–665.

Primary Structure of the cAMP-Dependent Phosphorylation Site of the Plasma Membrane Calcium Pump†

Peter H. James,‡ Martin Pruschy,‡ Thomas E. Vorherr,‡ John T. Penniston,§ and Ernesto Carafoli*,‡

Laboratory of Biochemistry, Swiss Federal Institute of Technology (ETH), CH-8092 Zurich, Switzerland, and Department of Biochemistry and Molecular Biology, Mayo Graduate School of Medicine, Rochester, Minnesota 55905

Received December 1, 1988; Revised Manuscript Received January 31, 1989

ABSTRACT: The primary structure of a region of the erythrocyte plasma membrane calcium pump which is phosphorylated by the cAMP-dependent protein kinase has been determined. The sequence is A-P-T-K-R-N-S-S(P)-P-P-P-S-P-D. The site is located between the calmodulin binding domain and the C-terminus of the ATPase. The ATPase is phosphorylated only at this site by the cAMP-dependent protein kinase, and the phosphorylation is inhibited by calmodulin. The effect of the phosphorylation is to decrease the K_m for Ca^{2+} of the purified ATPase from about 10 μM to about 1.4 μM and to increase the V_{max} of ATP hydrolysis about 2-fold.

It has become increasingly evident during the last few years that protein kinases modulate the activity of several, possibly most, membrane transport proteins, particularly in the plasma membrane. The calcium pump of plasma membranes has been shown to be activated by a cAMP-dependent protein kinase (Caroni & Carafoli, 1981; Neyses et al., 1985). This is analogous to the case of the (Na^+–K^+)-ATPase (Lin & Cantley, 1984) but is at variance to that of the sarcoplasmic reticulum calcium ATPase which is only activated indirectly by both cAMP- and calmodulin-dependent phosphorylation of the low molecular weight acidic proteolipid phospholamban (Tada & Katz, 1982). The phosphorylation of several other calmodulin-dependent enzymes has been demonstrated [e.g., myosin light chain kinase and phosphofructokinase (Lukas et al., 1986; Buschmeier et al., 1987)], and the sites of phosphorylation have been shown to be located near the calmodulin binding domains of these enzymes or within them. In these cases, the phosphorylation was shown to increase the K_m of the proteins for calmodulin, thus preventing activation. The site of phosphorylation in these enzymes is a serine-rich region immediately C-terminal to the calmodulin binding domain.

The sequences of the plasma membrane Ca^{2+} pumps from rat brain and human teratoma cells have recently been deduced from the corresponding cDNAs (Shull & Greeb, 1988; Verma et al., 1988). The sequence of the calmodulin binding domain has been determined by photoaffinity labeling and Edman degradation of the cross-linking peptides (James et al., 1988). The domain was found to be located near the C-terminus of the enzyme and to contain a serine-rich region homologous to the phosphorylation domains of the above-mentioned enzymes. The expectation was thus that a similar phosphorylation mechanism may occur in the plasma membrane Ca^{2+}-ATPase. The work presented here locates the site of cAMP-dependent phosphorylation in the ATPase: Contrary to expectation, it occurs at a site approximately 5 kDa C-terminal to the serine-rich region mentioned above. Its phosphorylation produces an activation of the purified ATPase and not an inhibition as seen with phosphofructokinase and myosin light chain kinase.

Materials and Methods

Staphylococcus aureus V8 protease was purchased from ICN Immunobiochemicals (Lisle, IL), ethanethiol (purissimum) was from Fluka AG (Buchs, Switzerland), and all HPLC solvents were from May and Baker (Dagenham, U.K.). The catalytic subunit of the cAMP-dependent protein kinase

† Supported by the Swiss Nationalfonds (Grant 3.531-0.86) and the National Institutes of Health (Grant GM 28835).
* Address correspondence to this author.
‡ Swiss Federal Institute of Technology.
§ Mayo Graduate School of Medicine.

0006-2960/89/0428-4253$01.50/0